Proceedings of the 8th International Symposium on

Advances in Civil and Environmental Engineering Practices for Sustainable Development

ACEPS - 2021

N_2O emission dynamics in differently-sized aggregates in agricultural soils

M.M.T. Lakshani[1], T.K.K. Chamindu Deepagoda[1], K. Smits[2], T.J. Clough[3], S. Thomas[4], B. Elberling[5]

[1]Dept. of Civil Engineering, Faculty of Engineering, University of Peradeniya, 20400 Peradeniya, Sri Lanka.
[2]Dept. of Civil Engineering, University of Texas, Arlington, TX 76019, USA.
[3]Dept. of Soil and Physical Sciences, Lincoln University, P.O. Box 85084, Lincoln, 7647, New Zealand.
[4]Plant & Food Research Lid, Gerald St, Lincoln 7608, New Zealand.
[5]Dept. of Geosicences and Natural Resources Management, Center for Permafrost (CENPERM), University of Copenhagen, Øster Volgade 10, DK-1350 Copenhagen, Denmark

ARTICLE INFO

Article history:
Received 31 July 2021
Revised 20 August 2021
Accepted 15 September 2021
Available online 07 October 2021

Keywords:
Soil aggregation
Soil-gas diffusivity
Soil moisture
N_2O fluxes

ABSTRACT

Grazed pastures can be introduced as a dominant source of nitrous oxide (N_2O), a high potent greenhouse gas. Although past studies have examined N_2O emissions in relation to soil physical properties, linking emissions with soil gas diffusivity (D_P/D_o) and its dependency on soil physical properties and soil moisture are lacking. This study to empirically correlated the N_2O emission dynamics in differently-sized aggregated soils using coarse (2–4 mm) and fine (< 0.2 mm) aggregates, and seven different combinations with varying fine aggregate fractions (F = 0, 0.2, 0.3, 0.4, 0.5, 0.6, 0.7, 0.8, and 1.0). Repacked samples of different combinations were saturated with KNO_3 (1800 µg mL^{-1}) solution and were systematically drained to nine different matric potentials (−1 kPa to −10 kPa), followed by an air-dry step (−30 kPa). At potential levels, N_2O flux and D_P/D_o were measured. The highest and lowest peak of N_2O were observed as F = 1.0 at D_P/D_o = 0.002 and F = 0.7 with the lowest D_P/D_o respectively.

1. INTRODUCTION

Grazed pasture is commonly enriched with N due to ruminant urine and fertilizer inputs, leading towards N_2O emission. The main release pathway of N_2O to the atmosphere occurs mainly as direct emissions from urine-affected soil or fertilized pasture soil (Oenema et al., 2005; Davidson, 2009). In response to these N inputs, N_2O is produced via a range of microbial transformation pathways including nitrification, nitrifier-denitrification, and denitrification (Kool et al., 2010; Clough et al., 2017; Wrage-Mönnig et al., 2018). Nitrous oxide (N_2O) is considered the single most important stratospheric ozone-depleting substance (Ravishankara et al., 2009) and it is the third most potent greenhouse gas after CO_2 and CH_4 with a global warming potential 298 times that of CO_2 over a 100-year horizon (Myhre et al., 2013). The provision of oxygen is a vital determinant of producing and consuming N_2O through the biological pathway (Wrage-Mönnig et al., 2018). Pasture soils get gradually transformed to aggregated bimodal structure due to higher carbon inputs such as livestock manure, soil-moisture dynamics, vegetation root penetration-exudate-entanglement, soil fauna, and microbial activities (Six et al., 2004; Ghezzehei, 2012). Well-structured pasture soil consists of two-pore regions; inter-aggregate regions which include the pore spaces between the aggregates, and intra-aggregate regions or the pore spaces within individual soil aggregates arranged hierarchically (Ghezzehei, 2012) and often assumed to have similar characteristics with important soil physical properties (Durner, 1994). Mitigation of N_2O emission depends on soil aeration occurs primarily via soil-gas diffusion.

Among bimodal pore structures, diffusion occurs predominantly inside the inter-aggregate pore space while intra-aggregate pores are filled with water. Further drying causes the draining of aggregates, enabling gas diffusion through intra-aggregate pores (Currie 1984). As confirmed by Balaine et al., (2013); Owens et al., (2017), D_p/D_o was found as a key predictor of N_2O fluxes by showing a strong relationship between D_p/D_o and N_2O fluxes. Moreover, Chamindu Deepagoda et al. (2018a) introduced a critical diffusivity window (D_p/D_o ~ 0.005–0.01) where peak N_2O for both intact and repacked soils, regardless of the soil texture, structure, and moisture status. It can be seen that most of the studies have not considered the potential effects of soil aggregation on soil-gas diffusivity on net N_2O fluxes. Hence in this study effect of soil aggregation on soil-gas diffusivity, and their combined effect on N_2O fluxes in pasture soils were investigated.

2. MATERIALS AND METHODS

2.1. Material characterization and sample preparation

In this study, Wakanui silt loam soil (classified as a Mottled Immature Pallic Soil (Hewitt, 2010)) was used from a grazed pasture at Lincoln University – New Zealand. This soil was characterized with an organic matter content of 52 mg g^{-1}, total N content of 2.8 mg g^{-1}, total C content of 29.7 mg g^{-1}, a C: N ratio of 10.6, and a pH of 5.9. First, the natural soil moisture was removed by air drying and then sieved to obtain the two desired fractions of coarse (2 – 4 mm) and fine (< 0.2 mm) aggregates. These coarse and fine aggregates were premixed and packed into stainless-steel rings with 7.3 cm internal dia., and 7.4 cm height, in three layers up to a depth of 5.0 cm, replicated three times according to the pre-decided mass fraction (mass ratio between fine and coarse aggregates adding up to unity). When preparing these combinations, care was taken not to crush aggregates during packing with an equal number of tappings (four) on the outside of the ring for each replicate. Before transferring the repacked cores onto tension tables, samples were saturated for 72 h by immersing the cores in a KNO_3 (1800 µg mL^{-1}) solution. The basic properties of each aggregate combination are shown in Table 1.

Table 1: The coarse (c) and fine (F) aggregate combination details

Combination	Fine fraction	P (g cm^{-3})	Φ (cm^3 cm^{-3})	D_p/D_o at Air dry stage#
C10F0	0.0	0.804	0.696	0.160
C8F2	0.2	0.866	0.673	0.110
C7F3	0.3	0.884	0.666	0.107
C6F4	0.4	0.878	0.669	0.122
C5F5	0.5	0.906	0.658	0.109
C4F6	0.6	0.933	0.648	0.100
C3F7	0.7	0.919	0.637	0.080
C2F8	0.8	0.919	0.653	0.085
C0F10	1.0	0.919	0.653	0.095

air dry at -30 kPa

2.2. Measurement methods

2.2.1. Aggregate size distribution

According to the extended modification of Rosin and Rammler (1933) two-region grain size distribution function by Chamindu Deepagoda et al. (2018b), the aggregate size distribution was analyzed and the mean aggregate size, D_{50}, of the characteristic aggregate size of the distribution was as mentioned below.

$$P(x) = 100\left[w\left(1 - e^{-ln2\left(\frac{x}{D_{50,c}}\right)^{\sigma_c}}\right) + (1 - w)\left(1 - e^{-ln2\left(\frac{x}{D_{50,f}}\right)^{\sigma_f}}\right)\right] \quad (1)$$

where, P(x) is a function of aggregate size, x (mm); $D_{50,c}$ and $D_{50,f}$ (mm) are corresponding mean aggregate sizes of coarse and fine aggregates, σ_c and σ_f (dimensionless) are empirical coefficients representing the spread of the distributions for coarse and fine aggregates, respectively, and the weighting parameter, w (dimensionless) is also used as the coarse aggregate fraction in the mixture. As per Eq. (2), the mean aggregate size for the entire distribution, D_{50}, can be determined as follows:

$$1 + 2w\left(e^{-ln2\left(\frac{D_{50}}{D_{50,f}}\right)^{\sigma_f}} - e^{-ln2\left(\frac{xD_{50}}{D_{50,c}}\right)^{\sigma_c}}\right) - 2e^{-ln2\left(\frac{D_{50}}{D_{50,f}}\right)^{\sigma_f}} = 0 \quad (2)$$

2.2.2. Soil gas diffusivity

Numerical characterization of the measured soil-gas diffusivity data was determined using the Density- Corrected (DC) model (Eq. (3)) developed by Chamindu Deepagoda et al. (2011) and measurements of D_p/D_o within the intra-aggregate region (mostly above pF 3 or −100 kPa) were not available to extend the model for a two-region D_p/D_o model as was done in previous studies (e.g., Jayarathne et al., 2019).

$$\frac{Dp}{Do} = 0.1\left[2\left(\frac{\varepsilon}{\emptyset}\right)^3 + 0.04\left(\frac{\varepsilon}{\emptyset}\right)\right] \quad (3)$$

where, D_p/D_o is the soil-gas diffusivity, ε is the soil air-filled porosity ($cm^3\ cm^{-3}$), and ϕ represents the soil total porosity ($cm^3\ cm^{-3}$).

2.2.3. Nitrous oxide flux measurement

After saturation, using tension tables, samples were drained to eight matric potentials (ψ) −1, −2, −3, −4, −5, −6, −8, and −10 kPa, followed by an air-dry step corresponding to a matric potential of −30 kPa. Drained samples to each matric potential were placed in a 1-L air-tight glass jar with a rubber septum lid and gas samples (10 mL) were extracted at 30 and 60 min after sealing the container. Gas samples were analyzed using the gas chromatography method with an electron capture detector; GC, SRI- 8610, Torrance, CA. Accordingly the proposed method by Hutchinson and Mosier (1981), a three-point linear regression method was used to calculate nitrous oxide emissions using ambient laboratory air samples and the samples which were taken at 30 and 60 min.

2.2.4. Soil gas diffusivity measurement

To obtain the soil gas diffusivity measurements, one chamber diffusion method which was presented by Taylor (1949), was used at each of the matric potential levels diffuse through the soil sample into the chamber. The values of D_p/D_o through repacked soil samples were calculated using the method developed by Currie (1960). Moreover, using a pre-calibrated galvanic O_2 sensor (KE-12, Figaro Inc.), increment of partial pressure of O_2 inside the chamber was monitored continuously. Chamber was flushed with 99.99% N_2 gas to make the chamber free of O_2 and then repacked soil sample was placed on the chamber allowing atmospheric O_2 to diffuse through the soil sample into the chamber. The values of D_p/D_o through repacked soil samples were calculated using the method developed by Currie (1960). Moreover, using a pre-calibrated galvanic O_2 sensor (KE-12, Figaro Inc.), increment of partial pressure of O_2 inside the chamber was monitored continuously.

2.3. Statistical analysis

Statistical analyses (ANOVA, regression, Pearson correlation) were performed using Minitab® 19. ANOVA was performed to test the effects of matric potential and fine fraction on nitrous dioxide flux emission.

3. RESULTS AND DISCUSSION

3.1. Aggregate size distribution and total porosity

Using the extended Rosin and Rammler (1933) two-region grain size distribution function (Eq. (1)), the measured aggregate size distribution (scattered points) and the corresponding simulated data (solid lines) are plotted on the same graph and the agreement between the measured and the model-determined coarse fraction (w) of each combination are shown in Figure 1a and 1b, respectively.

Except coarse (C10F0) and fine (C0F10) only combinations, all mass fractions show a bimodal grain size distribution. While C10F0 and C0F10 show uniformly distributed profiles, all other aggregate-distribution profiles present typical gap-graded distributions, demonstrating the mixing of two discrete size distributions.

The measured variation in size distribution well configured the extended Rosin and Rammler (1933) two-region grain

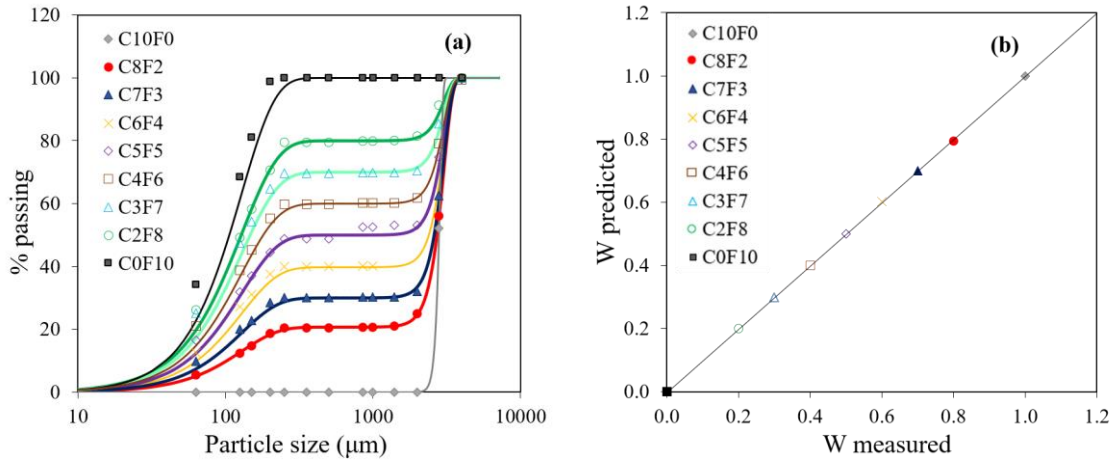

Figure 1: (a) Grain Size Distribution of aggregate combinations where F = fine fraction (< 0.2 mm) and C = coarse fraction (2 – 4 mm). Data points are measured values and solid lines are simulated using the extended Rosin Rammler two-region grain size distribution function, Eq. (1).

(b) Comparison between measured and simulated coarse fractions, where the solid line is the regression between measured and modelled variables.

size distribution function for each mass fraction combination with small RMSE values ranging from 0.11 to 4.81. As per Eq. 2, D_{50} was mathematically derived and the respective values for each combination are mentioned in Table (1). It can be seen a gradual increment of D_{50} values with the increase of the fraction of coarse aggregates.

While the uniformity coefficients Cu, for C10F0 as 1.11 and C0F10 as 3.12, (Cu < 4) show they were uniformly graded, the mixed aggregate soils show the gap gradation characteristics according to Cu values. Figure 2 depicts that the variation of measured total porosity with the fine fraction of the aggregate combinations and the coarse only combination (C10F0) represent the highest porosity value as 0.697.

It can be noted that the 0.637 as a minimum porosity value ($p < 0.001$) and measured porosity gradually decreased with the introduction of fine particles into mixtures. Theoretically, when the pore volume of coarse aggregates equates to the fine aggregate volume, finer aggregates fill the pores between coarser particles (Koltermann and Gorelick, 1995) and are further explained by the Porosity Exclusion Principle by Dexter (1988). Also, it can be generally observed the densest arrangement in C3F7 (Table 1) and further inclusion of fine aggregates into the mix resulted in increment of total porosity of C2F8 and C0F10. Normally, fine only aggregate mixture shows lower porosity than that of the coarse-only aggregate mix since when finer particles dominant in the mixture, coarse particles are scattered and supported by a matrix of finer grains. Hence interaggregate pores will subsist when only the inter-grain pore diameters are less than the fine-grain diameter.

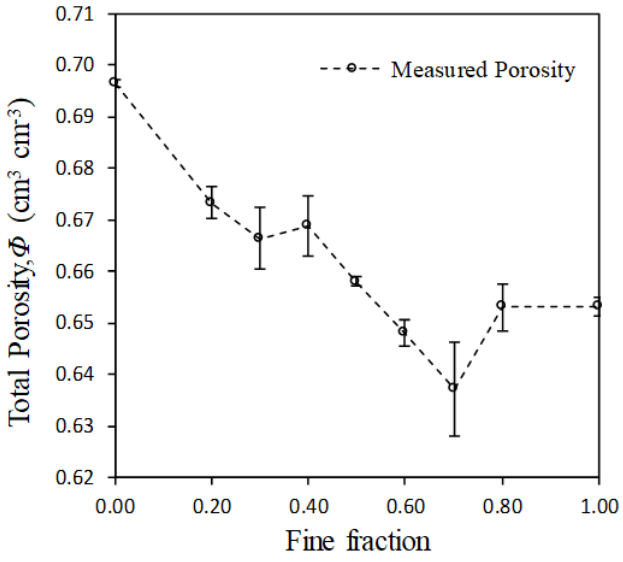

Figure 2: Variation in total porosity (Φ) with increasing fine aggregate fraction

3.2. Nitrous oxide fluxes and soil gas diffusivity

In this section, we considered measured N_2O net fluxes; the difference between the production of N_2O and its consumption within the soil aggregates, and the data represent the

fluxes corresponding to each matric suction and not the cumulative fluxes across different suction levels. The N_2O flux variation across all aggregate combinations with variation in D_p/D_o is shown by Figure 3. Soil Gas diffusivity (D_p/D_o); (ratio of air-filled porosity to the total porosity; ε/Φ) was the measure for all aggregate combinations at nine different matric potentials (-1 to −30 kPa). Diffusive flux of N_2O and O_2 into and out of the aggregate structure is unidirectional as stated by Schlüter et al., (2018). Since the D_p/D_o being a function of air-filled pore space and due to its moisture dependency, with the increasing soil moisture, N_2O fluxes also increased. Further, coarse-only (C10F0) aggregate with highest diffusivity generated lowest N_2O fluxes.

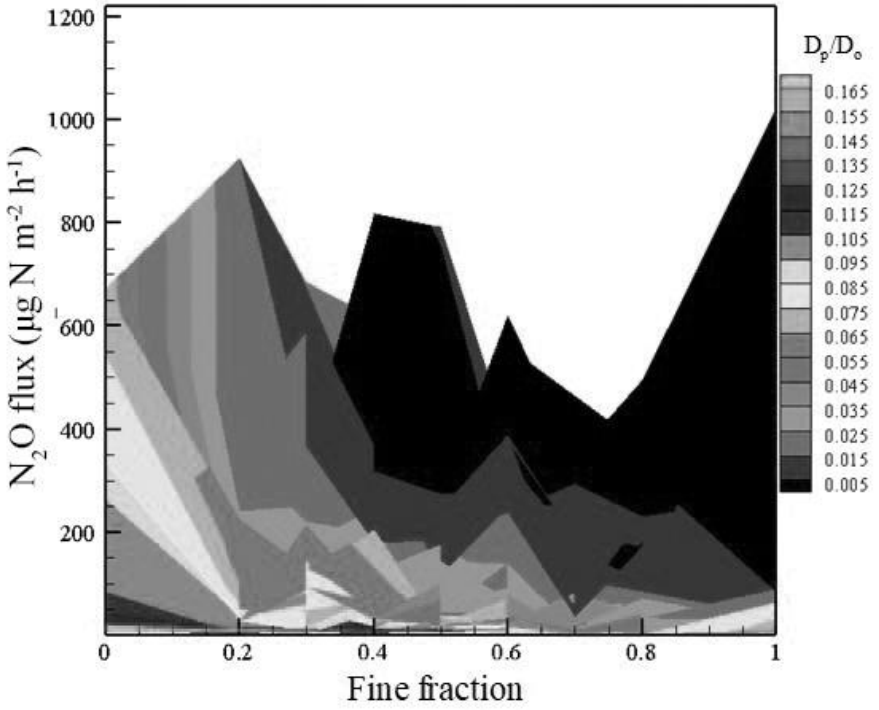

Figure 3: Variation in N_2O fluxes (vertical axis) for different fine fractions (horizontal axis) under different D_p/D_o variations

Moreover, coarse-only grain mixture gradually shows an increment in N_2O fluxes (25, 334, 418, and 673 µg N $m^{-2}h^{-1}$) with the decreasing of D_p/D_o values (0.1627, 0.0882, 0.0827, 0.0701) (see Figure 3). According to Diba et al., (2011), when the aggregate size is large, they tend to develop anaerobic conditions and Sexstone et al. (1985) used microelectrodes to demonstrate exponentially declined O_2 concentrations from the aggregate surface towards the middle. As Stein, (2019) noted, at the highest values of D_p/D_o, soil moistures were the lowest, and relatively low N_2O fluxes were observed in the C10F0 coarse only mixture likely due to microbial driven nitrification or nitrifier-denitrification processes producing N_2O. In addition, tortuosity of the diffusive pathway increases in response to the barrier for O_2 diffusion due to the packing of aggregates. Stepniewski (1981) and Balaine et al. (2016), who stated anaerobic conditions occur at D_p/D_o < 0.02 and N_2 production, denitrification, only occurred when repacked silt loam soil at D_p/D_o was < 0.005. Since likely, C10F0 were also anaerobic zones within aggregates where intra-aggregate diffusivity was indeed < 0.005 and the pF required to drain intra-aggregate pores (pF > 3) was not applied during N_2O flux measurement.

With the increase of intrusion fine grains to the soil mixtures, N_2O flux initially increased to 925 µg N $m^{-2}h^{-1}$ in C8F2 due to declination of D_p/D_o to < 0.015. With further increase of fine grains, it was clearly observed a lower magnitude two peaks under D_p/D_o value of 0.005 in C6F4 as 819 µg N $m^{-2}h^{-1}$ and C5F5 as 792 µg N $m^{-2}h^{-1}$, respectively. Minimum N_2O flux can be noted as 346 µg N $m^{-2}h^{-1}$ for C3F7 with the lowest diffusivity (D_p/D_o = 0.0015), (Fig 3; P < 0.05). This diminishing fluxed from C8F2 to C3F7 was due to a decrease in total porosity. Although the decrease in porosity should increase the anaerobic microsites and the potential for N_2O

production, according to the explanation; at 80% WFPS denitrification, N_2O production under acetylene, in fine aggregates (< 0.25 mm) was dominated by denitrification and O_2 diffusion was constrained into and around aggregates. In line with Sey et al. (2008), the lowest recorded N_2O peak in C3F7 can be ascribed to enhanced anaerobiosis promoting N_2O consumption via denitrification and produced N_2O can be partially or fully entrapped in result reducing N_2O emission from C8F2 to C3F7 (Letey et al., 1980; Clough et al., 2001; Balaine et al., 2016). Since the draining of aggregates was limited to a suction < pF 3 (100 kPa), the D_p/D_o measurements in this study were largely confined to the inter-aggregate pore space. It can be seen that all N_2O production in this study is within the D_p/D_o range of 0.001–0.015. According to the literature, Balaine et al. (2013) and Balaine et al. (2016) reported a highly sensitive range of D_p/D_o between 0.006 and 0.02 and lower and upper D_p/D_o limits of 0.005 and 0.02, respectively. Chamindu Deepagoda et al. (2019b) presented a "critical D_p/D_o window" of 0.005 ~ 0.01, which yielded peak N_2O fluxes. As reported by Stepniewski, (1981); Schjønning et al., (2003), the upper range value begins at a D_p/D_o of 0.02 occurs due to the onset of anaerobiosis with the lower range, D_p/D_o < 0.005, due to entrapment of N_2O and/or further reduction to N_2 (Balaine et al., 2016). In this study, it is worthy to mention that the altered pore network under pronounced soil aggregation has accompanied a shift in the diffusivity window (lower boundary) and N_2O flux peaks were observed over a WFPS range of 59.5 – 90.6%, while the majority of the peaks were observed at an average WFPS of 81.4%.

Also, the lowest peak N_2O flux of 34 µg N $m^{-2}h^{-1}$ in C3F7 occurred at a WFPS of 83.3% which is very close to the average WFPS where N_2O flux peaked. This further verifies that WFPS cannot always be used as a predictor of N_2O emissions, especially when comparing density varying soils (Farquharson and Baldock, 2008; Balaine et al., 2013). By considering the results of this study it has to be mentioned that when D_p/D_o increases with an increasing volume of air-filled pore space and developing connectivity of the functional gaseous pore network leads to minimizing N_2O emissions. Neverthelss, comparing the results of this study with other studies where undisturbed soils and field-scale measurements are involved, additional soil and environmental complexities may cause a considerable discrepancy with carefully controlled laboratory measurements in sieved and repacked soils, with aggregate sizes confined to < 0.2 mm and 2 – 4 mm fractions.

4. CONCLUSIONS

Under this study, the impact of differently-sized agricultural soils were investigated in relation to soil-gas diffusivity (D_p/D_o) and N_2O emission dynamics in repacked soil sampled from a perennial pasture site. Two aggregate fractions, coarse (2 – 4 mm) and fine (< 0.2 mm), and seven different combinations thereof were investigated. Increasing fine fraction enhanced nitrifier-denitrification, but further increasing fine fraction lowered N_2O peak emission likely due to a shift from nitrifier-denitrification to denitrification and entrapment Lowest N_2O peak occurred at 70% fine fraction (C3F7) with lowest diffusivity. Future studies are needed due to extend the data generated to generalize the analyses carried out in this research.

5. AKNOWLEDGEMENT

The authors gratefully acknowledge the financial support from Asia - Pacific Network for Global Change Research (APN) grant – CRRP2020-07MY-Deepagoda).

6. REFERENCES

Balaine, N., Clough, T.J., Beare, M.H., Thomas, S.M., Meenken, E.D., 2016. *Soil gas diffusivity controls N_2O and N_2 emissions and their ratio.* Soil Sci. Am. J. 80, 529-540.

Balaine, N., Clough, T.J., Beare, M.H., Thomas, S.M., Meenken, E.D., Ross, J.G., 2013. *Changes in relative gas diffusivity explain soil nitrous oxide flux dynamics*. Soil Sci. Am. J. 77:1496–1505. doi:10.2136/ sssaj2013.04.0141.

Chamindu Deepagoda T.K.K, Clough, T.J., Jayarathne, J.R.R.N., Thomas, S., Elberling, B., 2019b. *Soil-gas Diffusivity and Soil-Moisture effects on N_2O emissions from*

Repacked pasture soils. Soil Sci. Am. J. doi: 10.2136/sssaj2019.10.0405.

Chamindu Deepagoda, T.K.K., Clough, T.J., Thomas, S., Balaine, N., Elberling, B., 2018a. *Density effects on soil-water characteristics, soil-gas diffusivity, and emissions of N2O and N2 from a re-packed pasture soil*.Soil Sci. Am. J. doi: 10.2136/sssaj2018.01.0048.

Chamindu Deepagoda, T.K.K., Moldrup, P., Schjønning, P., de Jonge, L.W., Kawamoto, K., Komatsu, T., 2011. *Density-corrected models for gas diffusivity and air permeability in unsaturated soil*. Vadose Zone J. 10.2136/vzj2009.0137.

Chamindu Deepagoda, T.K.K., Smits, K., Jayarathne, J.R.R.N., Wallen, B.M., and Clough, T.J., 2018b. *Characterization of grainsize distribution, thermal conductivity, and gas diffusivity in variably saturated binary sand mixtures*. Vadose Zone J. 17: 180026.doi:10.2136/vzj2018.01.0026.

Clough, T.J., Lanigan, G.J., de Klein, C.A.M., Samad, Md. S., Morales, S.E., Rex, D., Bakken, L.R., Johns, C., Condron, L.M., Grant, J., Richards, K.G. 2017. *Influence of soil moisture on codenitrification fluxes from a urea-afected pasture soil*. Sci. Rep. Vol 7, article number 2185.

Clough, T.J., Sherlock, R.R., Cameron, K.C., Stevens, R.J., Laughlin, R.J., Müller, C. 2001. *Resolution of the ^{15}N balance enigma? Aus*. J. Soil Res. 39, 1419-1431. doi: 10.1071/SR00092.

Currie, J.A., 1984. *Gas diffusion through soil crumbs: the effects of compaction and wetting*. J. Soil Sci. 35, 1-10.

Currie, J.A., 1960. *Gaseous diffusion in porous media. Part 2*. – Dry granular materials.Brit. J. Appl. Phys. 11, 318–324.

Davidson, E.A., 2009. *The contribution of manure and fertilizer nitrogen to atmospheric nitrous oxide since 1860*. Nat. Geosci. 2, 659-662 · doi: 10.1038/ngeo608.

Dexter, A.R., 1988. *Advances in characterization of soil structure*. Soil Till. Res. 11, 199–238.

Diba, F., Shinizu, M., Hatano, R., 2011. *Effects of soil aggregate size, moisture content and fertilizer management on nitrous oxide production in a volcanic ash soil*. Soil Sci. Plant Nutri.57,733–747.

Durner, W. 1994. *Hydraulic conductivity estimation for soils with heterogeneous pore structure*. Water Resour. Res. 30, 211–223.

Farquharson, R., Baldock, J., 2008. *Concepts in modelling N2O emissions from land use Plant Soil*. 309, 147–167. doi:10.1007/s11104-007-9485-0.

Ghezzehei, T.A., 2012. Soil structure. In: Hung P, Li Y, Summer, M. (Eds). *Handbook of soil science, pp 1-17. Vol 2. Boca Raton: CRC Press* .

Hewitt, A. E., 2010. *New Zealand soil classification* (3rd edition). Lincoln, New Zealand: Manaaki Whenua Press.

Hutchinson, G.L., Mosier, A.R. 1981. *Improved soil cover method for field measurement of nitrous oxide fluxes*. Soil Sci. Soc. Am. J. 45, 311-316.

Jayarathne, J.R.R.N., Chamindu Deepagoda T.K.K., Clough T.J., Nasvi M.C.M., Thomas S., Elberling B. Smits, K., 2019. *Gas-Diffusivity Based Characterization of Aggregated Agricultural Soils*. Soil Sci. Soc. Am. J. doi.org/10.1002/saj2.20033.

Koltermann, C. E., Gorelick, S.M., 1995. *Fractional packing model for hydraulic conductivity derived from sediment mixtures*: Water Resour. Res. 31, 3283–3297. doi.org/10.1029/95WR02020.

Kool, D. M., Dolfing, J., Wrage, N., van Groenigen, J.W., 2010. *Nitrifier denitrification as a distinct and significant source of nitrous oxide from soil,* Soil Biol. Biochem. 43, 174–178.

Letey, J., Jury, W.A., Hadas, A., Valoras, N. 1980. *Gas diffusion as a factor in laboratory incubation studies on denitrification*. J. Environ. Qual. 9, 223-227. doi: 10.2134/jeq1980.00472425000900020012x.

Myhre, G., Shindell, D. Bréon, F.M., Collins, W., Fuglestvedt, J., Huang, J., Koch, D., Lamarque, J.F., Lee, D., Mendoza, B., Nakajima, T., Robock, A., Stephens, G., Takemura, T., Zhang, H. 2013. *Anthropogenic and Natural Radiative Forcing*. In: Climate Change 2013: The Physical Science Basis. Contribution of Working Group I to the Fifth Assessment Report of the Intergovernmental Panel on Climate Change [Stocker, T.F., D. Qin, G.K. Plattner, M. Tignor, S.K. Allen, J. Boschung, A. Nauels, Y. Xia, V. Bex and P.M. Midgley (eds.)]. Cambridge University Press,

Cambridge, United Kingdom and New York, NY, USA.

Oenema, O., Wrage, N., Velthof, G.L., Van Groenigen, J.W., Dolfing, J., Kuikman, P.J. *Trends in global nitrous oxide emissions from animal production systems*. 2005. Nutr. Cycl. Agroecosyst. 72, 51-65.doi: 10.1007/s10705-004-7354-2.

Owens, J., Clough, T.J., Laubach, J., Hunt, J.E., Venterea, R.T., 2017. *Nitrous Oxide Fluxes and Soil Oxygen Dynamics of Soil Treated with Cow Urine*. Soil Sci. Soc. Am. J. 81, 289–298. doi:10.2136/sssaj2016.09.0277.

Ravishankara, A.R., Daniel, J.S., Pormann, R.W., 2009. *Nitrous Oxide (N_2O): The Dominant Ozone-Depleting Substance Emitted in the 21st Century*. Science. 326, 123-125. DOI: 10.1126/science.1176985.

Rosin, P., Rammler, E., 1933. *Laws governing the fineness of powdered coal*. J. Inst. Fuel. 7, 29–36.

Schjønning, P., Thomsen, I.K., Moldrup, P., Christensen, B.T., 2003. *Linking Soil Microbial Activity to Water- and Air-Phase Contents and Diffusivities*. Soil Sci. Soc.Am. J. 67, 156–165.

Schlüter, S., Henjes, S., Zawallich, J., Bergaust, L., Horn, M., Ippisch, O., Vogel, H.J.,Dörsch, P., 2018. *Denitrification in soil aggregate analogues-effect of aggregate size and oxygen diffusion.* Front. Environ. Sci. 6, art.no. 17. https://doi.org/10.3389/fenvs.2018.00017.

Sey, B. K, Manceur, A.M., Whalen, J.K., Gregorich, E.G., Rochette, P. 2008. *Small-scale heterogeneity in carbon dioxide, nitrous oxide and methane production from aggregates of a cultivated sandy-loam soil*. Soil Biol. Biochem. 40, 2468–2473.

Sexstone, A.J., Revsbech, N.P., Parkin, T.B., Tiedje, J.M., 1985. *Direct measurement of oxygen profiles and denitrification rates in soil aggregates*. Soil Sci. Soc. Am. J. 49,645–651.

Six, J., Bossuyt, H., Degryze, S., Denef, K., 2004. *A history of research on the link between (micro)aggregates, soil biota, and soil organic matter dynamics*. Soil Till. Res. 79, 7–31. doi: 10.1016/j.still.2004.03.008.

Stein, L.Y., 2019. *Insights into the physiology of ammonia-oxidizing microorganisms*. Curr. Opin. Chem. Biol. 49, 9–15.

Stepniewski, W., 1981. *Oxygen diffusion and strength as related to soil compaction*: I. ODR. Pol. J. Soil Sci. 13, 3–13.

Taylor, S.A., 1949. *Oxygen diffusion in porous media as a measure of soil aeration*. Soil Sci. Soc. Am. J. 14, 55-61.

Wrage-Mönnig, N., Horn, M. A., Well, R., Müller, C., Velthof, G., Oenema, O., 2018. *The role of nitrifier denitrification in the production of nitrous oxide revisited*. Soil Biol. Biochem. 123, A3-A16. doi: 10.1016/j.soilbio.2018.03.020.